https://doi.org/10.5194/egusphere-2026-3656
Preprint. Discussion started: 9 July 2026

Asymmetric patterns of soil carbon mineralization during thaw slump recovery: Stable fast-pool size but rebounding decomposition rate

Hanhan Li[1,2,#,*], Tingan Dai[1,#], Danni Luo[1], Huan Wang[1], Min Xie[1], Yu Zhang[1,2], Xuegang Luo[1,2]

[1] *College of Life Science and Agri-forestry, Southwest University of Science and Technology, Mianyang 621010, China*

[2] *Engineering Research Center of Biomass Materials, Ministry of Education, College of Life Science and Agri-forestry, Southwest University of Science and Technology, Mianyang 621010, China*

[*]Corresponding author:

Hanhan Li: College of Life Science and Agri-forestry, Southwest University of Science and Technology, Mianyang 621010, China; e-mail: lihanhan@swust.edu.cn

[#] These authors contributed equally to this work.

https://doi.org/10.5194/egusphere-2026-3656
Preprint. Discussion started: 9 July 2026

Abstract

In areas of thermokarst landslides on the Qinghai-Tibet Plateau, the decline in soil CO_2 emissions over time is accompanied by a decrease in the proportion of active carbon and an increase in the proportion of inert carbon, suggesting that the soil organic carbon pool capacity and its mineralization rate may have changed. The lack of quantitative analysis regarding how actual active carbon pool capacity and mineralization rates regulate CO_2 emissions has led to some uncertainty in CO_2 emission estimates. In light of this, this study utilized a publicly available dataset of a 23-year recovery sequence from thermokarst landslides in the Qilian Mountains. By introducing a dual-pool index model, the cumulative CO_2 release process was decoupled into fast-pool capacity ($C_{0,fast}$) and fast-pool decomposition rate constant (k_{fast}), and their driving factors were identified using hierarchical variance decomposition (LMG) and partial least squares structural equation modeling (PLS-SEM). The results indicate that over the 23-year recovery period, $C_{0,fast}$ did not change significantly, while the turnover rate k_{fast} rebounded significantly. Furthermore, $C_{0,fast}$ was primarily driven by total microbial biomass ($r = 0.74$, $p = 0.003$), whereas k_{fast} was influenced by the chemical quality of organic carbon ($r = 0.60$, $p = 0.023$). Both LMG and PLS-SEM confirmed that the chemical quality of organic carbon is the primary driver of variation in k_{fast} (contributing approximately 30%), while microbial indicators contributed less than 15%. Furthermore, as the number of recovery years increased, $\delta^{13}C$ exhibited a significant negative trend ($\beta = -0.761$, $p < 0.001$), and both this trend and the subsequent recovery in pH were significantly correlated with k_{fast} ($r = -0.53$ and 0.51, respectively). Soil carbon mineralization during the recovery from thermokarst landslides exhibits an asymmetric pattern characterized by "stable pool capacity and a rebound in mineralization rate." This finding provides new kinetic evidence for assessing carbon dynamics following permafrost disturbance.

Keywords: thermokarst landslides; soil carbon mineralization; dual-pool model; active carbon pool; decomposition rate

https://doi.org/10.5194/egusphere-2026-3656
Preprint. Discussion started: 9 July 2026

1 Introduction

Permafrost regions store approximately 1,700 Pg of soil organic carbon, accounting for about half of the global soil carbon pool and representing one of the largest carbon reservoirs in terrestrial ecosystems(Schuur et al. 2015). Permafrost degradation triggered by climate warming is accelerating the release of this carbon in the form of CO_2 and CH_4, which may result in significant positive feedback on the global climate system(Schuur et al. 2015). To address this pressing issue, Earth System Models (ESMs) have gradually incorporated permafrost carbon cycle modules capable of modeling the vertical distribution of soil organic carbon, its temperature sensitivity, and the slow, gradual thawing process (Koven et al. 2013; Lawrence et al. 2015). However, recent model comparison studies have shown that predictions of permafrost carbon loss vary considerably across models; this uncertainty stems largely from inadequate representation of abrupt permafrost degradation processes—such as thermal karst—and the subsequent dynamics of ecosystem recovery (Schädel et al. 2016; Turetsky et al. 2020). Existing models typically assume that the decomposition rate constant of the carbon pool is a fixed value or is regulated solely by temperature and humidity; they have not yet accounted for the effects of substrate quality evolution and microbial functional recovery on turnover rates, making it difficult for the models to accurately predict the medium- to long-term trajectories of carbon dynamics following disturbances (Allison et al. 2010; Wieder et al. 2013).

Thermal melting and landslides are among the most prominent sudden manifestations of thermal karst; they can expose previously sequestered deep permafrost at the surface over periods ranging from months to years, radically altering soil hydrothermal conditions, substrate availability, and microbial community structure(Olefeldt et al. 2016). In the recovery sequence following such disturbances, understanding how the soil's carbon mineralization potential evolves hinges on answering two interrelated yet potentially independent questions: Does the capacity of the active carbon pool change systematically with the duration of recovery? And does the decomposition rate constant of the active carbon pool change synchronously? Traditional views often implicitly assume that the decline in soil respiration following disturbance stems primarily from the depletion of the active carbon pool—that is, a synchronous decrease in both capacity and rate(Alvarez & Alvarez 2000). However, if the active carbon pool receives continuous replenishment during recovery (e.g., from root exudates or microbial residues), its capacity may remain stable or even rebound; simultaneously, if the chemical quality of the substrate

https://doi.org/10.5194/egusphere-2026-3656
Preprint. Discussion started: 9 July 2026

improves or microbial metabolic activity increases, the decomposition rate constant may also change independently. Whether capacity and rate evolve synchronously or whether an asymmetric recovery pattern exists is a core question that remains to be tested.

The dual-pool index model provides an effective quantitative tool for distinguishing between changes in capacity and rate. By decoupling the cumulative CO_2 release curve into two independent parameters—the fast-pool (activated carbon) capacity ($C_{0,fast}$) and the fast-pool decomposition rate constant (k_{fast})—this model can separately assess the contributions of substrate quantity and substrate quality/microbial activity to carbon mineralization and has been widely applied in studies of agricultural and forest soils(Collins et al. 2000; Davidson & Janssens 2006). Applying this model to the recovery sequence of thermokarst landslides in permafrost will help determine whether the active carbon pool capacity and decomposition rate constant evolve synergistically or respond divergently along the recovery gradient, thereby providing key information for improving the parameterization of carbon pool turnover in Earth System Models (ESMs).

Divergent responses in capacity and rate may be independently regulated by distinct environmental factors. The chemical quality of organic carbon, such as the alkyl carbon/oxygen alkyl carbon ratio (A/O ratio) determined by solid-state ^{13}C NMR, typically indicates the degree of decomposition and chemical persistence of organic matter; traditionally, a high A/O ratio implies a lower decomposition rate(Baldock et al. 1997). However, during the late stages of recovery, the substantial accumulation of microbial residues can simultaneously contribute alkyl carbon and partially hydrolyzable active components, which may alter the relationship between the A/O ratio and the decomposition rate(Kallenbach et al. 2016; Liang et al. 2017). At the same time, total microbial biomass often determines the upper limit of the active carbon pool's potential capacity, while abiotic factors—such as shifts in $\delta^{13}C$ and changes in pH during the recovery process—may also indirectly regulate turnover rates by influencing microbial metabolic efficiency(Ehleringer et al. 2000; Wang et al. 2003). The relative importance of these environmental factors—as well as their synergistic and antagonistic pathways—regarding activated carbon pool capacity and degradation rate constants has not yet been quantitatively distinguished in thermoklinic landslide recovery sequences, resulting in a lack of evidence for parameterizing substrate-microbial-environmental interactions in models.

Hence, this study utilized a publicly available dataset of a 23-year recovery sequence for thermokarst landslides in the Qilian Mountains (Mu & Mu, 2024). Using cumulative mineralization data

https://doi.org/10.5194/egusphere-2026-3656
Preprint. Discussion started: 9 July 2026

from 248 days of laboratory cultivation, this study employed a dual-pool exponential model to fit the variations in $C_{0,fast}$ and k_{fast} within the recovery sequence. By integrating hierarchical variance decomposition (LMG) and partial least squares structural equation modeling (PLS-SEM), the study quantitatively analyzed the independent and synergistic pathways through which factors such as carbon chemical quality, microbial biomass, $\delta^{13}C$, and pH influence these parameters. This study aims to investigate the evolution patterns of the soil active carbon pool capacity and decomposition rate constants during the recovery from thermokarst collapse, as well as their environmental regulatory mechanisms, thereby providing empirical constraints and process insights to improve the parameterization of permafrost carbon dynamics in Earth system models.

2 Materials and Methods

2.1 Data Sources:

The data for this study were obtained from a dataset publicly released by Mu & Mu 2025 (2025)(Mu & Mu 2025) on the PANGAEA data repository (https://doi.org/10.1594/PANGAEA.970424), which contains comprehensive observations of soil properties, carbon composition, microbial communities, and potential CO_2 production rates for a typical thermokarst landslide sequence in the Qilian Mountains region (37°28′N, 100°17′E) on the northern margin of the Tibetan Plateau. The original study established four treatment plots in the thermokarst landslide area(Mu et al. 2024): control (natural meadow without landslides); active phase (approximately 1 year after the landslide); mid-phase (approximately 12 years after the landslide); and stable phase (approximately 23 years after the landslide). Three plots were established for each treatment, and samples were collected from the 0–15 cm (topsoil) and 15–30 cm (subsoil) layers. After passing through a 2-mm sieve and removing gravel and roots, the samples were subjected to further analysis. Key variables in the dataset are listed in Table S1 in the Appendix.

2.2 Dual-Pool Index Mineralization Model

2.2.1 Model Development

To distinguish the decomposition kinetics of different activated carbon pools, the 248-day cumulative CO_2 release curves for each soil sample were fitted to two models:

https://doi.org/10.5194/egusphere-2026-3656
Preprint. Discussion started: 9 July 2026

Single-pool model(Stanford & Smith 1972):

$$C(t) = C_0(1 - e^{-kt}) \quad (1)$$

Where C(t) is the cumulative CO_2-C release at time t (mg CO_2-C /g SOC), C_0 is the total potential mineralizable carbon, and k is the first-order decomposition rate constant (d^{-1}).

Two-pool model(Andren & Paustian 1987):

$$C(t) = C_{0,fast}\left(1 - e^{-k_{fast}t}\right) + C_{0,slow}(1 - e^{-k_{slow}t}) \quad (2)$$

where $C_{0,fast}$ and $C_{0,slow}$ represent the sizes of the fast and slow pools, respectively, and kfast and kslow are the corresponding decomposition rate constants ($k_{fast} > k_{slow}$).

Model parameters were estimated using the scipy.optimize.curve_fit function in Python via nonlinear least squares, with a lower bound of 0 for the parameters and an upper bound of 1.0 d^{-1} for the single-pool rate constants. and for the two-pool model, the upper limits for k_{fast} and k_{slow} are set to 1.0 d^{-1} and 0.5 d^{-1}, respectively. The maximum number of iterations is set to 10,000 to ensure convergence; the rationality of these upper limits is confirmed through sensitivity analysis and ANOVA (Tables S2–S4, Note S1).

2.2.2 Model Selection

For each sample, the corrected Akaike Information Criterion (AICc, Equation 3) is calculated based on the optimal fit. The model with the lower AICc value is selected as the optimal model for that sample; when $\Delta AICc \leq 2$, the single-pool model is selected in accordance with the principle of parsimony (Hurvich & Tsai 1989; Symonds & Moussalli 2011). From the optimal model, the fast pool capacity $C_{0,fast}$, the slow pool capacity $C_{0,slow}$, the total mineralizable carbon $C_{0,total} = C_{0,fast} + C_{0,slow}$, the fast pool decomposition rate constant k_{fast}, and the slow pool decomposition rate constant k_{slow} are extracted as kinetic parameters for subsequent analysis. The goodness of fit for all samples is evaluated using the coefficient of determination R^2 and the root mean square error (RMSE).

$$AICc = nln\left(\frac{SSE}{n}\right) + 2K + \left(\frac{2K(K+1)}{n-K-1}\right) \quad (3)$$

Where n is the number of observations, SSE is the sum of squared errors, and K is the number of model parameters (K = 3 for a single reservoir, K = 5 for a dual reservoir; includes an estimate of the error variance).

2.2.3 Sensitivity Analysis of Parameter Upper Limits

https://doi.org/10.5194/egusphere-2026-3656
Preprint. Discussion started: 9 July 2026

To examine whether kfast's response to recovery duration depends on artificially set parameter upper limits, a sensitivity analysis of kfast's response to recovery duration was conducted. In the two-reservoir model, the upper limits of k_{fast} were set to 0.5, 1.0, 2.0, and 5.0 d^{-1} (with the upper limit of k_{slow} fixed at 0.5 d^{-1}), and multi-source fitting was performed again for all samples. A two-way analysis of variance (Years × Depth) was performed on the k_{fast} values obtained for each set of upper limits. If the effect of recovery duration (Years) remained significant ($p < 0.05$) across all upper limit settings, this indicates that the core conclusions are not affected by the choice of parameter upper limits.

2.3 Statistical Analysis

2.3.1 Analysis of Variance and Effect Sizes

A two-way analysis of variance (ANOVA) was used to test the effects of collapse duration and soil depth, as well as their interaction, on the kinetic parameters ($C_{0,fast}$; k_{fast}; $C_{0,slow}$; k_{slow}; $C_{0,total}$). The model is as follows (Hector et al. 2010):

$$Y \sim Years + Depth + Years \times Depth \quad (4)$$

A Type II sum-of-squares decomposition was used, implemented via the “ols” and “anova_lm” functions in “statsmodels”.

When the interaction term is not significant ($p > 0.05$), Tukey HSD multiple comparisons are performed for statistically significant main effects (Tukey 1949); when the interaction term is significant, simple effect tests and multiple comparisons are conducted separately at each level of the respective variables. To supplement the information from the significance tests and quantify the practical significance of the treatment effects, Cohen’s d effect size for paired comparisons is calculated (Fritz et al. 2012):

$$d = \frac{\overline{X_1} - \overline{X_2}}{S_{pooled}}, S_{pooled} = \sqrt{((n_1 - 1)S_1^2 + (n_1 - 1)S_2^2)/(n_1 + n_2 - 2)} \quad (5)$$

According to Cohen’s (2016) (Cohen 2016) criteria, |d| = 0.2, 0.5, and 0.8 represent small, medium, and large effect sizes, respectively.

2.3.2 Bivariate Correlation Analysis

To reveal the relationships between kinetic parameters ($C_{0,fast}$; k_{fast}; $C_{0,slow}$; k_{slow}; $C_{0,total}$) and soil chemistry (SOC, TN, C/N, DOC, O-alkyl C, alkyl C, alkyl carbon/oxygen alkyl carbon ratio (O/C)), as

https://doi.org/10.5194/egusphere-2026-3656
Preprint. Discussion started: 9 July 2026

well as microbial properties (total PLFA, fungal/ bacterial PLFA ratio, BG enzyme, and NAG enzyme), Pearson correlation coefficients were calculated for all pairwise combinations of variables. To assess the uncertainty of the correlation coefficients, bootstrap resampling (n = 5,000, random seed 42) was performed for each correlation coefficient to estimate its 95% confidence interval. The correlation matrix was visualized as a heatmap, with significance levels labeled as $p < 0.05$, $p < 0.01$, and $p < 0.001$.

2.3.3 Principal Component Analysis (PCA) of the Chemical Characteristics of Organic Matter

To eliminate the strong multicollinearity among the carbon functional group indicators (O-alkyl C, alkyl C, and O/C ratio) obtained from solid-state ^{13}C NMR spectra, this study employed standardized principal component analysis for dimensionality reduction. In a Python 3.13.2 environment, the scikit-learn library was used to standardize the variables using Z-scores, and extract principal components. The first two principal components (PC1 and PC2) were retained based on the criteria that their eigenvalues were greater than 1 or that they collectively explained more than 85% of the variance. PC1 primarily characterizes the relative abundance gradient of carbohydrates and aromatic carbon, while PC2 reflects the differences between alkyl carbon and carboxyl/carbonyl carbon. The scores of these two principal components serve as multidimensional quantitative indicators of organic matter chemical quality and are used in subsequent hierarchical variance decomposition and structural equation modeling.

2.3.4 Hierarchical Variance Decomposition (LMG)

To quantify the independent contributions of soil physicochemical properties and microbial attributes to mineralization kinetics, the Lindeman–Merenda–Gold (LMG) method was employed for hierarchical variance decomposition (Grömping 2007). Unlike traditional regression coefficients, the LMG algorithm effectively eliminates biases caused by variable orderaveraging the marginal R^2 increments for each variable across all possible ordering sequences in the model. Using the fast-pool decomposition rate constant k_{fast} and the initial carbon content of the fast pool $C_{0,fast}$ as response variables, we constructed multiple linear regression models comprising the following three categories of explanatory variables: (I) Basic soil properties, including soil organic carbon (SOC), total nitrogen (TN), carbon-to-nitrogen ratio (C/N), dissolved organic carbon (DOC), pH, and $\delta^{13}C$ values; (II) Chemical characteristics of organic matter, namely the scores PC1 and PC2 extracted via PCA; (III) Microbial characteristics, covering total PLFA biomass, the fungal/bacterial PLFA ratio, and β-glucosidase activity.

https://doi.org/10.5194/egusphere-2026-3656
Preprint. Discussion started: 9 July 2026

Using custom Python code, we calculated the mean increase in R^2 for all possible variable sequences, obtained the percentage of variance explained by each factor for each response variable, and finally presented their relative importance using horizontal bar charts.

2.3.5 Partial Least Squares–Structural Equation Modeling

To reveal the causal pathways through which the age of collapse indirectly influences decomposition rates via chemical and microbial pathways of organic matter, a principal component-based partial least squares–structural equation model was constructed (Wold 1982). Given the limited sample size (n = 23), principal component analysis (PCA) was used to generate latent variables: recovery time was represented by the ordinal coding of landslide duration (0 = control, 1 = 1 year, 2 = 12 years, 3 = 23 years) as a single manifest variable; carbon chemical quality was derived from O-alkyl C, Alkyl C, and the A/O ratio via the first principal component extracted by PCA; the microbial community was derived from total PLFA, the F/B ratio, and the PLFA of fungi, bacteria, and actinomycetes via the first principal component extracted by PCA; k_{fast} was directly based on measured values. Path assumptions included that recovery duration directly influences carbon chemical quality and the microbial community, that carbon chemical quality influences the microbial community and k_{fast}, that the microbial community influences k_{fast}, and that recovery duration directly influences k_{fast}. Model parameters were estimated iteratively using ordinary least squares regression. Bootstrap resampling (n = 5,000, random seed 42) was employed to obtain 95% confidence intervals and standard errors for path coefficients, with significance determined using a Z-test ($|Z| > 1.96$ corresponds to $p < 0.05$). The model's predictive ability was assessed using the Q^2 statistic, and its robustness was verified through a permutation test (10,000 repetitions). Based on this, a mediation analysis was conducted to decompose the total effect of restoration duration on k_{fast} into a direct effect, an indirect effect via organic carbon chemistry, an indirect effect via microbial communities, and a serial indirect effect of the two. The indirect effects and their confidence intervals were simultaneously reported using the Bootstrap percentile method.

2.3.6 Supplementary Analysis of δ13C and pH

To verify the robustness of the relationship between carbon mass and decomposition rate and to explore the possible moderating effect of pH, this study further incorporated supplementary analyses of soil organic carbon stable isotopes ($\delta^{13}C$) and pH. First, Pearson correlation tests were conducted to

https://doi.org/10.5194/egusphere-2026-3656
Preprint. Discussion started: 9 July 2026

examine the relationships between $\delta^{13}C$ and the Alkyl/O-alkyl ratio as well as k_{fast}, to assess the feasibility of using $\delta^{13}C$ as a proxy for the degree of organic matter decomposition; A two-way analysis of variance (recovery years × soil layer) was conducted to test for differences in pH across treatments, and the correlation between pH and k_{fast} was calculated. Subsequently, a linear moderation model, k_{fast} ~ Alkyl/O-alkyl + pH + Alkyl/O-alkyl × pH, was constructed to examine whether pH moderates the effect of organic carbon quality on decomposition rate. Based on this, $\delta^{13}C$ and pH were incorporated into the existing PLS-SEM framework as two new latent variables—carbon isotope (Carbon Isotope, unmanifest variable) and soil acidity (Acidity, unmanifest variable), respectively. It was hypothesized that both restoration duration and organic carbon chemical quality influence $\delta^{13}C$, and that pH has direct effects on the microbial community and k_{fast}; The estimation of all path coefficients and the Bootstrap significance test methods were identical to those described in Section 2.3.5.

All statistical analyses and graph generation were performed in a Python 3.13.2 environment, primarily using libraries such as pandas, numpy, scikit-learn, scipy, statsmodels, and matplotlib/seaborn (see Appendix Table S2 for details).

3 Results

3.1 Asymmetric Dynamics of Soil Carbon Pools and Decomposition Rates During Restoration

Based on the criterion of ΔAICc > 2, a two-pool model was selected for 22 of the 23 samples, while only one sample (1 HT3 A1, 23-year-old topsoil) used a single-pool model (Table S3),the cumulative CO_2-C release curves for all samples fit the models well (Fig. 1). $C_{0,fast}$ did not differ significantly across different restoration years (ANOVA, $F_{3,14} = 3.20$, $p = 0.056$), but was significantly higher in the topsoil than in the subsoil ($p = 0.001$; Fig. 2a). In contrast, k_{fast} exhibited a significant effect of restoration year ($F_{3,14} = 5.11$, $p = 0.013$) . Post hoc tests indicated that k_{fast} in the 23-year-old soil was significantly higher than that in the 1-year-old ($p = 0.006$) and 12-year-old ($p = 0.029$) soils (Fig. 2b). Cohen's d values for the 23-year-old soil compared to the 1-year-old, 12-year-old, and control samples were 1.94, 1.45, and 1.67, respectively, all indicating a large effect size (Table S4). This exhibited an asymmetric pattern characterized by a stable $C_{0,fast}$ and an increasing k_{fast}. Neither $C_{0,slow}$ nor k_{slow} showed significant changes across the recovery years ($p > 0.3$), indicating that the recovery process primarily reshaped the turnover characteristics of the active carbon fraction. Correlation analysis showed (Fig S1; Table S5) that k_{fast} was

https://doi.org/10.5194/egusphere-2026-3656
Preprint. Discussion started: 9 July 2026

significantly positively correlated with the alkyl carbon/oxygen alkyl carbon ratio (A/O ratio) (r = 0.60, p = 0.023) and significantly negatively correlated with $C_{0,fast}$ (r = –0.67, p = 0.009). It is worth noting that the positive correlation between k_{fast} and the A/O ratio contradicts the conventional wisdom that "the poorer the carbon quality, the slower the decomposition." SOC and TN were not significantly correlated with k_{fast} (p > 0.05), whereas total PLFA and the fungus-to-bacteria ratio (F/B) were significantly positively correlated with $C_{0,fast}$ (r = 0.74, p = 0.003; r = 0.62, p = 0.017). This suggests that microbial biomass primarily controls the capacity of the soil fast pool rather than its decomposition rate, and also indicates that the regulatory factors for pool capacity and decomposition rate may have independent components.

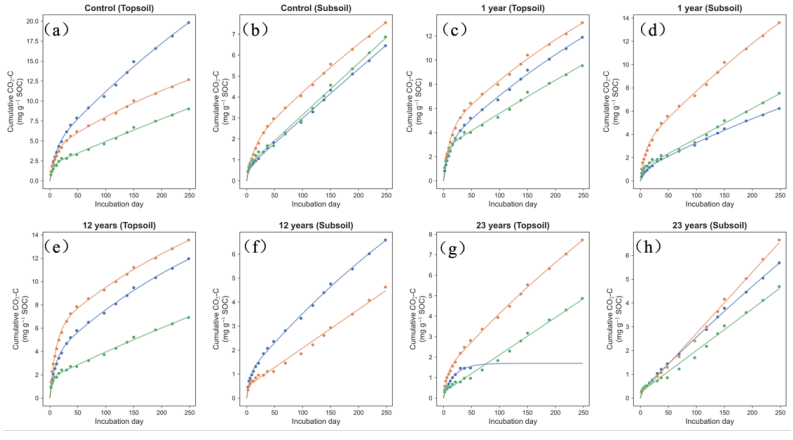

Fig 1. Cumulative CO_2-C emissions (mg g^{-1} SOC) over 248 days of incubation from topsoil and subsoil across a thaw slump recovery chronosequence on the northeastern Qinghai-Tibetan Plateau.

Panels (a–h) represent soil layers under different land-use durations: (a, b) Control, (c, d) 1 year, (e, f) 12 years, and (g, h) 23 years, with topsoil (left) and subsoil (right) shown for each stage. Data points indicate observed cumulative CO_2-C values at each time point.

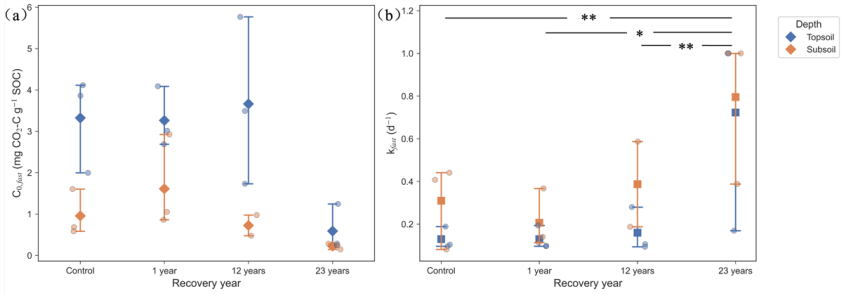

https://doi.org/10.5194/egusphere-2026-3656
Preprint. Discussion started: 9 July 2026

Fig 2. Fast SOC pool parameters across a thaw slump chronosequence (northeastern Qinghai-Tibetan Plateau).

(a) Initial fast *C* content ($C_{0,fast}$; mg CO_2-C g^{-1} SOC) in topsoil (blue) and subsoil (orange); (b) Fast C decomposition rate (k_{fast}; d^{-1}) for both depths. （*, p< 0.05; **, p< 0.01）denote significant topsoil - subsoil differences.

3.2 Key Drivers of Rapid Storage Decomposition Rates

PCA first condenses the chemical structure of organic carbon into two orthogonal dimensions (Fig. 3a): PC1 (load: Alkyl C = 0.599, A/O = 0.643, O-alkyl C = −0.477) characterizes the "alkylation/refinement" gradient, while PC2 (load: O-alkyl C = 0.855, Alkyl C = 0.487) characterizes the "abundance of oxygen-containing groups/degree of oxidation" gradient. Based on this, LMG decomposition (Fig. 3b) shows that the chemical quality of organic carbon is the primary factor determining k_{fast}, with PC1 contributing 23.7%—the single largest contributor—and PC2 contributing 6.2%, together accounting for nearly 30%; In contrast, the combined independent contributions of microbial indicators (total PLFA 2.1%, BG 2.0%, F/B 5.0%) totaled less than 15%, indicating that the spatial variation in k_{fast} is primarily controlled by "substrate chemical quality" rather than "microbial abundance." The PLS-SEM model explains 56.8% of the variance in k_{fast} (R^2 = 0.568). Restoration duration has a significant direct effect on k_{fast} (β = 0.697, p = 0.005; Fig. 4; Table S6), and also acts through two indirect pathways: restoration duration positively influences organic carbon chemistry (β = 0.541, p = 0.035), which in turn positively influences k_{fast} (β = 0.607, p = 0.008); the restoration duration negatively affects microbial biomass (β = –1.158, p = 0.022), but the path from microbial biomass to k_{fast} is not significant (β = –0.188, p = 0.141). Mediation analysis revealed (Table S7) that both the indirect effect of organic carbon chemistry (0.328) and the total indirect effect (0.639, 95% CI [0.094, 1.499]) were significant, and the substitution test confirmed the non-randomness of the aforementioned key path (p < 0.05; Table S8). Q2 values indicated predictive correlations among the endogenous latent variables (organic carbon chemistry: 0.173; microbial biomass: 0.013; k_{fast}: 0.349; Table S9).

https://doi.org/10.5194/egusphere-2026-3656
Preprint. Discussion started: 9 July 2026

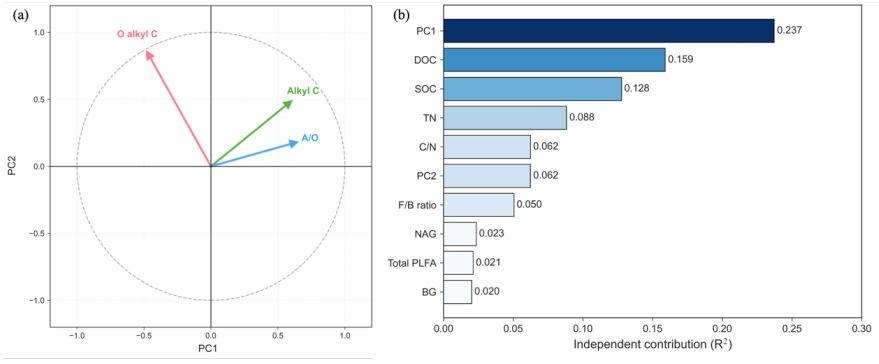

Fig 3. Drivers of fast carbon pool decomposition (k_{fast}) derived from LMG analysis and the linkage between carbon fractions and decomposition rates.

(a) Principal component analysis (PCA) biplot revealing the covariance among soil carbon fractions (O-alkyl C and Alkyl C) and stoichiometric ratios (A/O). (b) LMG analysis quantifying the independent contribution (R^2) of potential predictors to the variability of the k_{fast}.

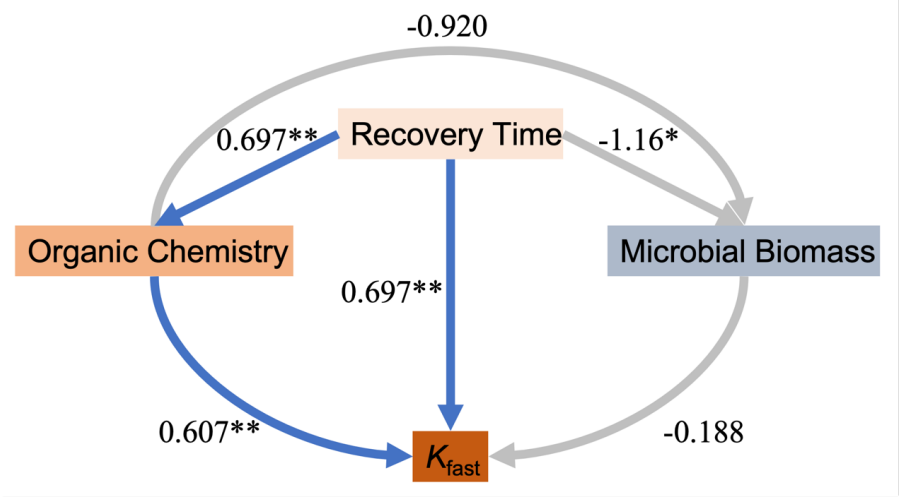

Fig 4. Structural equation modeling (SEM) path diagram illustrating the drivers of fast carbon decomposition rate ($k_{0,fast}$) during thermokarst slump succession.

Arrows indicate hypothesized causal relationships with standardized path coefficients labeled. Blue lines represent positive effects, while gray lines represent negative effects; asterisks denote statistical significance (* p<0.05, ** p<0.01, *** p<0.001).

3.3 Validation via $\delta^{13}C$ and pH Analysis

As the recovery period increased, the $\delta^{13}C$ of soil organic carbon showed a significantly negative

https://doi.org/10.5194/egusphere-2026-3656
Preprint. Discussion started: 9 July 2026

trend (β = –0.761, p < 0.001) and was significantly negatively correlated with both the A/O ratio (r = –0.66, p = 0.007) and k_{fast} (r = –0.53, p = 0.042) (Fig. S2). Soil pH initially decreased and then increased after disturbance (years of recovery: p = 0.031; depth: p = 0.027) and was positively correlated with k_{fast} (r = 0.51, p = 0.018; Fig. S3). Extended PLS-SEM analysis revealed that carbon isotopes harmed k_{fast} (β = –0.572, p = 0.025), acidity had a positive effect (β = 0.515, p = 0.041), while the direct path of organic carbon chemistry on k_{fast} remained significant (β = 0.607, p = 0.008; Table S10). Soil moisture content decreased with restoration duration (p < 0.001) but was not significantly correlated with k_{fast}; there were no systematic differences in clay and silt content, and these were unrelated to k_{fast}, ruling out the possibility of texture and moisture as major confounding variables (Table S11).

3.4 Robustness Tests

When the upper limits of the dual-reservoir model parameters were altered (k_{fast} capped at 5 d^{-1}, k_{slow} at 2 d^{-1}), less than 18% of k_{fast} values reached the original upper limit, and none of the k_{slow} values did; furthermore, two-way ANOVA indicated that the significant effect of restoration duration on k_{fast} held under all upper limits (Tables S12–14; Note S1). After excluding single-pool samples from the subsequent dual-pool model, the ANOVA p-values, correlation coefficients, LMG contributions, and PLS SEM path coefficients were nearly identical between the full dataset and the dual-pool-only dataset (Table S15). This confirms that the conclusions were not influenced by the upper limits of k_{fast} and k_{slow} or by model selection, ensuring the methodological reliability of the two core findings: the “effect of recovery years on k_{fast}” and the “dominant role of organic carbon chemistry.”

4 Discussion

4.1 Changes in CO_2 Release Potential During the Recovery Process

The results from the dual-reservoir model show that 23 years after recovery from a thermokarst collapse, C0,fast has not changed significantly, while k_{fast} has rebounded significantly (Salome et al. 2010). This asymmetric pattern cannot be explained by the traditional view that “a decline in CO_2 release results from the depletion of easily decomposable carbon.” The long-term stability of $C_{0,fast}$, combined with the significant recovery of kfast, collectively indicate that the fast pool consistently receives a continuous supply of carbon throughout the recovery process and that its decomposition capacity continues to strengthen as environmental conditions improve (Kuzyakov 2010). From a mechanistic

https://doi.org/10.5194/egusphere-2026-3656
Preprint. Discussion started: 9 July 2026

perspective, the carbon balance in the fast pool may be maintained by two types of supply processes: First, exogenous supply driven by vegetation recovery, whereby increased vegetation cover in the later stages of recovery directly transfers continuously fixed photosynthetic carbon to the soil's active carbon pool via root exudates, fine root turnover, and mycorrhizal symbionts (Godbold et al. 2006); second, endogenous supply driven by the microbial carbon pump, whereby microorganisms, while utilizing readily degradable substrates, convert a portion of the carbon into biomass; upon cell death, this biomass re-enters the soil carbon pool in the form of cell debris (such as cell wall fragments and extracellular polymers), providing a continuous internal carbon source for the fast pool (Liang et al. 2017; Miltner et al. 2012). Although residual carbon is generally relatively persistent, a portion of it—such as peptidoglycan, phospholipids, and certain polysaccharides—has a relatively short average residence time and can re-enter the fast pool during turnover (Gunina & Kuzyakov 2015). Therefore, the stability of the fast pool capacity does not stem from the cessation of consumption but rather from the attainment of a dynamic equilibrium between consumption and replenishment. The subsequent rebound in k_{fast} must be understood in terms of microbial functional activation. In the early stages of recovery, deteriorating substrate quality, declining pH, and a sharp decrease in microbial biomass collectively inhibited degradation activity; however, in the middle to late stages of recovery, as fresh carbon input increased and environmental conditions improved, the metabolic activity of the microbial community was reactivated (Bardgett & Van Der Putten 2014; Dacal et al. 2019). It is worth noting that the recovery of k_{fast} does not require the full restoration of total microbial biomass, as evidenced by the lack of a significant correlation between total PLFA and k_{fast} (Zak et al. 2011). This reflects that adjustments in microbial metabolic strategies play a dominant role in regulating degradation rates. Even under conditions where community size is limited, key functional groups can significantly enhance overall degradation capacity by upregulating the synthesis and activity of extracellular enzymes (Burns et al. 2013). Specifically, extracellular enzyme-producing fungi and actinomycetes may, during the late stages of recovery, prioritize allocating more energy to enzyme production rather than biomass accumulation, thereby achieving high carbon turnover efficiency with fewer cells (Štursová et al. 2012). Furthermore, improved substrate availability can further amplify this effect by altering microbial carbon utilization efficiency (CUE): when readily available substrates are abundant, microorganisms tend to lower their CUE and increase respiratory flux, releasing more carbon as CO_2 rather than using it for biomass synthesis (Manzoni et al. 2012; Sinsabaugh et al. 2013). Therefore, the regulation of rapid carbon pool

https://doi.org/10.5194/egusphere-2026-3656
Preprint. Discussion started: 9 July 2026

decomposition rates should be expanded from a single static attribute, "substrate quality" to a dynamic coupled process involving "substrate availability and microbial metabolic strategies," in which the response of metabolic strategies largely determines the sensitivity of carbon release to environmental conditions.

4.2 Chemical Mechanisms of Organic Carbon Maintenance and Rate Enhancement

Both LMG decomposition and PLS-SEM analysis consistently indicate that an increase in the A/O ratio is the primary chemical driver for the recovery of k_{fast}. However, as an indicator of the degree of organic matter decomposition, the A/O ratio is typically negatively correlated with decomposition rates, which stands in stark contrast to the positive correlation observed in this study (Baldock et al. 1997; Feng & Simpson 2007). The key to resolving this paradox lies in understanding the dual chemical sources of the rising A/O ratio during the recovery process and the differential decoupling of these sources from carbon turnover. The alkyl carbon region (0–45 ppm) defined by NMR is not a chemically homogeneous entity: it includes both plant-derived long-chain lipids and cutin (highly recalcitrant) as well as microbial-derived branched-chain fatty acids, peptidoglycans, and some protein side chains (relatively easily degradable) (Kögel-Knabner 2017). In the late stages of recovery, the continuous production and selective preservation of microbial residues can enhance alkyl carbon signals; however, a significant proportion of this carbon still belongs to active components that can be rapidly mineralized (Kallenbach et al. 2016; Miltner et al. 2012). Therefore, the overall increase in the A/O ratio may reflect the accumulation of carbon of microbial origin rather than an increase in the overall persistence of the carbon pool. This interpretation reconciles the apparent contradiction between a "high A/O ratio" and a "high k_{fast}": the A/O ratio here is not an inhibitor of decomposition, but rather a concomitant marker of active carbon components (hydrolyzable carbon in microbial residues) (Liang et al. 2017). PCA analysis further reveals this functional decoupling of chemical structures: PC1 (alkylation gradient) and PC2 (O-alkyl C abundance) are mutually orthogonal, indicating that the abundance of readily degradable carbon (such as O-alkyl C) does not decline linearly with the progression of immobilization. This implies that the stability of the fast pool capacity has an independent chemical basis: the continuous supply of O-alkyl C (Helfrich et al. 2007). Root exudates and fresh litter, which serve as inputs for vegetation recovery in the late restoration phase, are rich in carbohydrates and amino acids, directly replenishing the oxygen-alkyl carbon pool (Gunina & Kuzyakov 2015). At the same time, the turnover of oxygen-alkyl carbon (e.g.,

https://doi.org/10.5194/egusphere-2026-3656
Preprint. Discussion started: 9 July 2026

polysaccharides) within the microbial residue carbon pool also helps maintain its proportion within the overall carbon pool (Jones et al. 2009). This chemical structural characteristic of "decoupling between immobilization and oxidation" enables the fast pool to retain sufficient active components to maintain its capacity and support a high decomposition rate, even amid "deteriorating" chemical quality in the overall carbon pool. Functional differentiation among microorganisms further reinforces this explanation: the positive correlation between total PLFA and $C_{0,fast}$ is independent of k_{fast}, suggesting that microorganisms influence pool capacity through residue deposition and decomposition rates through metabolic activity (Bailey et al. 2002). The F/B and A/O ratios exhibit a trend toward negative correlation ($r = –0.46$, $p = 0.082$), suggesting that fungi may exert a leverage effect in the formation of microbial residues: fungal hyphal residues are rich in chitin and melanin and are chemically more refractory, yet their turnover process can still contribute specific active components to the fast pool (Kögel-Knabner 2017). Furthermore, changes in the abundance of actinomycetes may also influence the composition of alkyl carbon, as actinomycetes are known to be major contributors to microbial residues; their cell walls contain branched-chain fatty acids that fall within the alkyl carbon region in NMR spectra (Mahieu et al. 1999). The decoupling pattern between the stability of $C_{0,fast}$ and the increase in k_{fast} may stem from the accumulation of carbon from microbial residues, which raises the overall A/O ratio while simultaneously supplying active carbon components to the fast pool, driving a rebound in the rate; meanwhile, vegetation carbon input and microbial residue turnover jointly maintain the abundance of oxygenated alkyl carbon, ensuring the stability of the pool capacity (Cotrufo et al. 2013; Sokol et al. 2019). Microorganisms play a dual role in this process as both "carbon pool contributors" and "metabolic executors"; the decoupling of these two functions indicates that the regulation of carbon pool capacity and decomposition rates undergoes a certain degree of functional differentiation during the recovery process.

4.3 Multiple Mechanisms Driving the Recovery of k_{fast}

$\delta^{13}C$ and pH further reveal the synergistic effects of fresh carbon input and improvements in the abiotic environment. The $\delta^{13}C$ of soil organic carbon becomes increasingly negative with increasing restoration duration (from −25.6‰ to −26.2‰) and is significantly negatively correlated with k_{fast}. This trend provides a key isotopic fingerprint for distinguishing the sources of active carbon (Werth & Kuzyakov 2010). The $\delta^{13}C$ of C_3 plants typically ranges from −28‰ to −25‰; microorganisms preferentially utilize ^{12}C during decomposition, leading to an enrichment of ^{13}C in residual carbon by

https://doi.org/10.5194/egusphere-2026-3656
Preprint. Discussion started: 9 July 2026

approximately 1–3‰ (O'Leary 1988; Šantrůčková et al. 2000). Therefore, if active carbon in the late stages of restoration primarily originates from the microbial residue cycle, $\delta^{13}C$ should tend toward positive values. The observed trend is the opposite, strongly supporting the input of fresh plant carbon—particularly the direct contribution of root exudates—that is depleted in ^{13}C. Root exudates are rich in organic acids, sugars, and amino acids, and their $\delta^{13}C$ is typically more negative than that of the root tissue as a whole, as they are rapidly synthesized from recent photosynthetic products and have not undergone sufficient isotopic fractionation (Werth & Kuzyakov 2010). Once these exudates enter the soil, they are rapidly utilized by microorganisms, lowering the overall soil $\delta^{13}C$ while providing highly bioavailable substrates for the fast pool (Ehleringer et al. 2000; Kuzyakov 2010). The role of fresh carbon input is not limited to direct replenishment; it also accelerates the decomposition of indigenous organic matter through an "activation effect." Low-molecular-weight organic compounds in root exudates provide readily available energy to microorganisms, triggering the synthesis of extracellular enzymes, which, in turn, synergistically decompose pre-existing, more recalcitrant organic carbon in the soil (Blagodatskaya & Kuzyakov 2008). The negative correlation ($r = -0.67$) between k_{fast} and $C_{0,fast}$ observed in this study reflects precisely this "high-quality, rapid turnover" configuration: at sites with frequent fresh carbon inputs and strong priming effects, highly bioavailable substrates are sufficient to support a high k_{fast} without relying on a large $C_{0,fast}$ stock (Cotrufo et al. 2013; Manzoni et al. 2012). Therefore, the rebound in k_{fast} during the late recovery phase is not merely a result of cumulative carbon accumulation, but rather an acceleration of carbon turnover driven by the dual mechanisms of direct replenishment and stimulated decomposition. The recovery of soil pH provides critical abiotic support for the aforementioned carbon processes. Thermal melting and landslides exposed deep acidic parent material, causing a post-disturbance decline in surface soil pH; as the recovery period progressed, the neutralization of organic acids and mineral weathering led to a gradual recovery of pH (Olefeldt et al. 2016; Walker et al. 2010). pH may influence decomposition rates through two pathways: first, as a direct response to physiological activity. Low pH acts as a stressor on microorganisms, inhibiting the secretion of extracellular enzymes; a rise in pH, however, significantly increases the specific activity of microbial biomass per unit, compensating for the numerical deficit during the community recovery phase and driving a rapid rebound in decomposition function (Rousk et al. 2010; Sinsabaugh et al. 2008). Second, it involves the indirect optimization of resource availability. Near-neutral conditions not only increase phosphorus availability to alleviate nutrient limitations but also expose more binding sites by dissociating

https://doi.org/10.5194/egusphere-2026-3656
Preprint. Discussion started: 9 July 2026

organic-mineral complexes, thereby enhancing substrate accessibility (Grybos et al. 2007). The positive correlation between pH and $k_{fast,}$ along with the independent effect of acidity observed in PLS-SEM, collectively indicates that the more favorable chemical environment during the late recovery phase compensates for the shortage of microbial biomass, enabling "low abundance, high activity" functional output.

4.4 Implications for Assessing the Carbon-Climate Feedback of Thermokarst Slides and Improving Models

The kinetic decoupling identified in this study, in which the fast pool capacity remains stable while the release rate accelerates. In contrast, the release rate accelerates, offering valuable insights into the carbon-climate feedback of thermokarst slides and for parameterizing Earth System Models (ESMs). In terms of feedback assessment, inferring that the risk of carbon release has been eliminated solely based on the lower in-situ flux observed during the late recovery phase may underestimate the long-term emission potential (Turetsky et al. 2020). k_{fast} approached control levels 23 years into recovery, indicating that microbial decomposition function had largely recovered; the persistently negative $\delta^{13}C$ values confirmed that fresh carbon continued to enter the fast pool and was rapidly turned over, implying that photosynthetic carbon input from vegetation could be re-released through decomposition in the fast pool. Therefore, the long-term carbon budget should be viewed as a dynamic equilibrium between vegetation carbon input and soil carbon release, rather than a simple process of natural decay following disturbance-induced release (Abbott et al. 2016; Schuur et al. 2009). For ESMs, the decomposition rate constant should not depend solely on temperature and moisture. In this study, the A/O ratio independently explained approximately 30% of the variance in k_{fast}; based on this, we propose introducing a substrate quality adjustment function to correct the fast pool rate constant: $k_{fast} = k_{base} \times (A/O)^{\gamma}$, where k_{base} is the baseline rate controlled by physical factors such as temperature and moisture, and γ is the substrate quality sensitivity index (Schädel et al. 2014). This parameterization scheme aids in tracking medium- to long-term trajectories of carbon turnover following thermokarst disturbances.

4.5 Limitations of the Study

Through a dual-reservoir decoupling analysis, this study revealed an asymmetric pattern of "stable reservoir capacity and recovering rates" in the recovery sequence of thermokarst landslides and constructed a carbon turnover framework centered on substrate supply and microbial functional

https://doi.org/10.5194/egusphere-2026-3656
Preprint. Discussion started: 9 July 2026

regulation. However, the study still has certain limitations. The limited sample size (n = 23) may obscure more subtle phasic changes in the recovery process. Future studies should increase the number of sampling sites across a larger spatial scale and cover a denser recovery time series (e.g., at 3–5-year intervals) to accurately capture the inflection point of k_{fast} recovery and its coupling with vegetation recovery stages. Furthermore, the inferences regarding carbon sources and microbial functions in this study primarily rely on indirect indicators such as $\delta^{13}C$, the A/O ratio, and PLFA. Future research could incorporate microbial residue biomarkers (e.g., amino sugars) and metagenomic data to directly quantify the abundance and expression of carbon-degrading functional genes, thereby advancing the current framework from the phenomenological level to the process level and providing a more robust mechanistic foundation for predicting carbon dynamics in alpine ecosystems.

5 Conclusions

By decoupling dual carbon pool kinetics, this study revealed an asymmetric pattern of "stable capacity and recovering rate" in soil carbon mineralization during the recovery sequence following a thermokarst collapse, indicating that the recovery of active carbon pools after permafrost disturbance is not dominated by a single substrate-consumption pathway. Organic carbon chemical quality, as the primary driver of the recovery in decomposition rates, exhibits a positive effect accompanied by the accumulation of alkyl carbon. This suggests that during the later stages of recovery, the carbon pool may have maintained an adequate supply of active components through the synergistic effects of plant input and in situ transformation, even as the overall chemical composition tended toward alkylation, thereby avoiding mineralization stagnation caused by substrate depletion. Furthermore, the synergistic effect of isotopic signals from fresh plant carbon inputs and the recovery of pH further indicates that the recovery of decomposition rates results from the combined effects of carbon supply, improved chemical quality, and optimization of the abiotic environment, rather than a simple recovery of microbial biomass. These findings expand the framework for understanding carbon dynamics following thermoklinic landslides from a "substrate depletion" model to a multi-process coupling perspective that integrates carbon input, chemical reorganization, and functional reactivation, thereby providing a kinetic perspective for assessing and predicting carbon dynamics in disturbed alpine ecosystems.

Data Availability

https://doi.org/10.5194/egusphere-2026-3656
Preprint. Discussion started: 9 July 2026

The soil property, carbon composition, microbial community, and incubation data used in this study are publicly available from PANGAEA (Mu & Mu, 2024; https://doi.org/10.1594/PANGAEA.970424), licensed under CC BY 4.0. All original data collection and processing methods are described in Mu et al. (2024).

All code used for data preprocessing, statistical analyses, and figure generation is written in Python 3.13.2. The full analysis code is publicly available at GitHub: https://github.com/jewiei/Decoupling-of-fast-pool-size-and-decomposition-rate-explains-declining-soil-CO2-release/commit/1fc167c497b0a90ee62ea5aae9eab10f0092a770 . The repository includes detailed documentation to ensure reproducibility of all results.

Author Contributions

H.H. Li, T.A. Dai conceived and designed the project. T.A. Dai, D.N. Luo, and H. Wang developed the modelling framework and performed the analyses. Y. Zhang and M. Xie participated in result interpretation and discussion. H.H. Li and X.G. Luo drafted the initial manuscript. All authors reviewed and edited the manuscript. H.H. Li and T.A. Dai are the co-first authors.

Competing interests

The contact author has declared that none of the authors has any competing interests.

Disclaimer

Publisher's note: Copernicus Publications remains neutral with regard to jurisdictional claims made in the text, published maps, institutional affiliations, or any other geographical representation in this paper. The authors bear the ultimate responsibility for providing appropriate place names. Views expressed in the text are those of the authors and do not necessarily reflect the views of the publisher.

Acknowledgments

We would like to thank those who have shared datasets publicly available on the PANGAEA data repository (https://doi.org/10.1594/PANGAEA.970424), particularly Mei Mu, Cuicui Mu, and their co-authors, whose published data made this study possible.

https://doi.org/10.5194/egusphere-2026-3656
Preprint. Discussion started: 9 July 2026

Financial support

This work was supported by Natural Science Foundation of Sichuan Province, China (grant number 2026NSFSC0979) and Southwest University of Science and Technology PhD Fund (grant number 23zx7141).

Reference

Abbott, B. W., Jones, J. B., Schuur, E. A., Chapin, F. S., Bowden, W. B., Bret-Harte, M. S., Epstein, H. E., Flannigan, M. D., Harms, T. K., Hollingsworth, T. N.: Biomass offsets little or none of permafrost carbon release from soils, streams, and wildfire: an expert assessment. Environmental Research Letters., 11, 034014, https://doi.org/10.1088/1748-9326/11/3/034014, 2016.

Allison, S. D., Wallenstein, M. D., Bradford, M. A.: Soil-carbon response to warming dependent on microbial physiology. Nature Geoscience., 3, 336-340, https://doi.org/10.1038/ngeo846, 2010.

Alvarez, R., Alvarez, C.: Soil organic matter pools and their associations with carbon mineralization kinetics. Soil Science Society of America Journal., 64, 184-189 , https://doi.org/10.2136/sssaj2000.641184x, 2000.

Andren, O., Paustian, K.: Barley straw decomposition in the field: a comparison of models. Ecology., 68, 1190-1200, https://doi.org/ 10.2307/1939203, 1987.

Bailey, V. L., Smith, J. L., Bolton, J. H.: Fungal-to-bacterial ratios in soils investigated for enhanced C sequestration. Soil Biology and Biochemistry., 34, 997-1007, https://doi.org/10.1016/s0038-0717(02)00033-0, 2002.

Baldock, J. A., Oades, J., Nelson, P., Skene, T., Golchin, A., Clarke, P.: Assessing the extent of decomposition of natural organic materials using solid-state 13 C NMR spectroscopy., Soil Research 35, 1061-1084, https://doi.org/10.1071/s97004, 1997.

Bardgett, R. D., Van, D., Putten, W. H.: Belowground biodiversity and ecosystem functioning. Nature 515(7528): 505-511, https://doi.org/10.1038/nature13855, 2014.

Blagodatskaya, E., Kuzyakov, Y.: Mechanisms of real and apparent priming effects and their dependence on soil microbial biomass and community structure: critical review. Biology and Fertility of Soils., 45, 115-131, https://doi.org/10.1007/s00374-008-0334-y, 2008.

Burns, R. G., DeForest, J. L., Marxsen, J., Sinsabaugh, R. L., Stromberger, M. E., Wallenstein, M. D., Weintraub, M. N., Zoppini, A.: Soil enzymes in a changing environment: Current knowledge and

https://doi.org/10.5194/egusphere-2026-3656
Preprint. Discussion started: 9 July 2026

591 future directions. Soil Biology and Biochemistry., 58, 216-234,
592 https://doi.org/10.1016/j.soilbio.2012.11.009, 2013.
593 Cohen, J.: A power primer, https://doi.org/10.1037/14805-018, 2016.
594 Collins, H., Elliott, E., Paustian, K., Bundy, L., Dick, W., Huggins, D., Smucker, A., Paul, E.: Soil carbon
595 pools and fluxes in long-term corn belt agroecosystems. Soil biology and Biochemistry., 32, 157-
596 168, https://doi.org/10.1016/s0038-0717(99)00136-4, 2000.
597 Cotrufo, M. F., Wallenstein, M. D., Boot, C. M., Denef, K., Paul, E.: The Microbial Efficiency-Matrix
598 Stabilization (MEMS) framework integrates plant litter decomposition with soil organic matter
599 stabilization: do labile plant inputs form stable soil organic matter? Global Change Biology., 19,
600 988-995, https://doi.org/10.1111/gcb.12113, 2013.
601 Dacal, M., Bradford, M. A., Plaza, C., Maestre, F. T., García-Palacios, P.: Soil microbial respiration
602 adapts to ambient temperature in global drylands. Nature Ecology & Evolution., 3, 232-238 ,
603 https://doi.org/10.1038/s41559-018-0770-5, 2019.
604 Davidson, E. A., Janssens, I. A.: Temperature sensitivity of soil carbon decomposition and feedbacks to
605 climate change. Nature., 440, 165-173, https://doi.org/10.1038/nature04514, 2006.
606 Ehleringer, J. R., Buchmann, N., Flanagan, L. B.: Carbon isotope ratios in belowground carbon cycle
607 processes. Ecological Applications., 10, 412-422, https://doi.org/10.1890/1051-
608 0761(2000)010[0412:ciribc]2.0.co;2, 2000.
609 Feng, X., Simpson, M. J.: The distribution and degradation of biomarkers in Alberta grassland soil
610 profiles. Organic Geochemistry., 38, 1558-1570 ,
611 https://doi.org/10.1016/j.orggeochem.2007.05.001, 2007.
612 Fritz, C. O., Morris, P. E., Richler, J. J.: Effect size estimates: current use, calculations, and interpretation.
613 Journal of experimental psychology: General., 141, 2 , https://doi.org/10.1037/a0024338, 2012.
614 Godbold, D. L., Hoosbeek, M. R., Lukac, M., Cotrufo, M. F., Janssens, I. A., Ceulemans, R., Polle, A.,
615 Velthorst, E. J., Scarascia-Mugnozza, G., De, A. P.: Mycorrhizal hyphal turnover as a dominant
616 process for carbon input into soil organic matter. Plant and Soil., 281, 15-24 ,
617 https://doi.org/10.1007/s11104-005-3701-6, 2006.
618 Grömping, U.: Estimators of relative importance in linear regression based on variance decomposition.
619 The American Statistician., 61, 139-147 , https://doi.org/10.1198/000313007x188252, 2007.
620 Grybos, M., Davranche, M., Gruau, G., Petitjean, P.: Is trace metal release in wetland soils controlled by

https://doi.org/10.5194/egusphere-2026-3656
Preprint. Discussion started: 9 July 2026

organic matter mobility or Fe-oxyhydroxides reduction? Journal of colloid and interface science., 314, 490-501, https://doi.org/10.1016/j.jcis.2007.04.062, 2007.

Gunina, A., Kuzyakov, Y.: Sugars in soil and sweets for microorganisms: review of origin, content, composition and fate. Soil Biology and Biochemistry., 90, 87-100, https://doi.org/10.1016/j.soilbio.2015.07.021, 2015.

Hector, A., Von, Felten. S., Schmid, B.: Analysis of variance with unbalanced data: an update for ecology & evolution. Journal of animal ecology., 79, 308-316, https://doi.org/10.1111/j.1365-2656.2009.01634.x, 2010.

Helfrich, M., Flessa, H., Mikutta, R., Dreves, A., Ludwig, B.: Comparison of chemical fractionation methods for isolating stable soil organic carbon pools. European Journal of Soil Science., 58, 1316-1329, https://doi.org/10.1111/j.1365-2389.2007.00926.x, 2007.

Hurvich. C. M., Tsai, C. L.: Regression and time series model selection in small samples. Biometrika., 76, 297-307, https://doi.org/10.1093/biomet/76.2.297, 1989.

Jones, D. L., Nguyen, C., Finlay, R. D.: Carbon flow in the rhizosphere: carbon trading at the soil–root interface. Plant and Soil., 321, 5-33, https://doi.org/10.1007/s11104-009-9925-0, 2009.

Kallenbach, C. M., Frey, S. D., Grandy, A. S.: Direct evidence for microbial-derived soil organic matter formation and its ecophysiological controls. Nature communications., 7, 13630 , https://doi.org/10.1038/ncomms13630, 2016.

Kögel-Knabner, I.: The macromolecular organic composition of plant and microbial residues as inputs to soil organic matter: Fourteen years on. Soil Biology and Biochemistry, 105, A3-A8, https://doi.org/10.1016/j.soilbio.2016.08.011, 2017.

Koven, C., Riley, W., Subin, Z., Tang, J., Torn, M., Collins, W., Bonan, G., Lawrence, D., Swenson, S.: The effect of vertically resolved soil biogeochemistry and alternate soil C and N models on C dynamics of CLM4. Biogeosciences., 10, 7109-7131, https://doi.org/10.5194/bg-10-7109-2013, 2013

Kuzyakov, Y.: Priming effects: interactions between living and dead organic matter. Soil Biology and Biochemistry., 42, 1363-1371, https://doi.org/10.1016/j.soilbio.2010.04.003, 2010.

Lawrence, D. M., Koven, C. D., Swenson, S. C., Riley, W. J., Slater, A.: Permafrost thaw and resulting soil moisture changes regulate projected high-latitude CO2 and CH4 emissions. Environmental Research Letters., 10, 094011, https://doi.org/10.1088/1748-9326/10/9/094011, 2015.

https://doi.org/10.5194/egusphere-2026-3656
Preprint. Discussion started: 9 July 2026

Liang, C., Schimel, J. P., Jastrow, J. D.: The importance of anabolism in microbial control over soil carbon storage. Nature microbiology., 2, 1-6, https://doi.org/10.1038/nmicrobiol.2017.105, 2017.

Mahieu, N., Randall, E., Powlson, D.: Statistical analysis of published carbon-13 CPMAS NMR spectra of soil organic matter. Soil Science Society of America Journal., 63, 307-319 , https://doi.org/10.2136/sssaj1999.03615995006300020008x, 1999.

Manzoni, S., Taylor, P., Richter, A., Porporato, A., Ågren, G. I.: Environmental and stoichiometric controls on microbial carbon-use efficiency in soils. New phytologist., 196, 79-91, https://doi.org/10.1111/j.1469-8137.2012.04225.x, 2012.

Miltner., A., Bombach, P., Schmidt-Brücken, B., Kästner, M.: SOM genesis: microbial biomass as a significant source. Biogeochemistry., 111, 41-55, https://doi.org/10.1007/s10533-011-9658-z, 2012.

Mu, M., Mu, C.: Soil properties, carbon composition, microbial community, and potential CO2 production from a typical thaw slump on the northern Qinghai-Tibet Plateau. In. PANGAEA, https://doi.org/10.1594/PANGAEA.970424, 2025.

Mu, M., Mu, C., Liu, H., Zhang, C., Jia, Y., Lei, P., Peng, X.: Decline of CO2 Release During the Evolution of the Thaw Slump on the Northern Qinghai-Tibet Plateau. Journal of Geophysical Research: Biogeosciences., 129, e2024JG008162, https://doi.org/10.1029/2024JG008162, 2024.

O'Leary, M. H.: Carbon isotopes in photosynthesis. Bioscience., 38, 328-336, https://doi.org/10.2307/1310735, 1988.

Olefeldt, D., Goswami, S., Grosse, G., Hayes, D., Hugelius, G., Kuhry, P., McGuire, A. D., Romanovsky, V., Sannel, A. B. K., Schuur, E.: Circumpolar distribution and carbon storage of thermokarst landscapes. Nature communications., 7, 13043, https://doi.org/10.1038/ncomms13043, 2016

Rousk, J., Bååth, E., Brookes, P. C., Lauber, C. L., Lozupone, C., Caporaso, J. G., Knight, R., Fierer, N.: Soil bacterial and fungal communities across a pH gradient in an arable soil. The ISME journal., 4, 1340-1351, https://doi.org/10.1038/ismej.2010.58, 2010.

Salome, C., Nunan, N., Pouteau, V., Lerch, T. Z., Chenu, C.: Carbon dynamics in topsoil and in subsoil may be controlled by different regulatory mechanisms. Global Change Biology., 16, 416-426, https://doi.org/10.1038/ismej.2010.58, 2010.

Šantrůčková, H., Bird, M., Lloyd, J.: Microbial processes and carbon-isotope fractionation in tropical and temperate grassland soils. Functional Ecology., 14, 108-114, https://doi.org/10.1046/j.1365-2435.2000.00402.x, 2000.

https://doi.org/10.5194/egusphere-2026-3656
Preprint. Discussion started: 9 July 2026

Schädel, C., Bader, M. K-F., Schuur, E. A., Biasi, C., Bracho, R., Čapek, P., De, Baets. S., Diáková, K., Ernakovich, J., Estop-Aragones, C.: Potential carbon emissions dominated by carbon dioxide from thawed permafrost soils. Nature climate change., 6, 950-953, https://doi.org/10.1038/nclimate3054, 2016.

Schädel, C., Schuur, E. A., Bracho, R., Elberling, B., Knoblauch, C., Lee, H., Luo, Y., Shaver, G. R., Turetsky, M. R.: Circumpolar assessment of permafrost C quality and its vulnerability over time using long-term incubation data. Global change biology., 20, 641-652, https://doi.org/10.1111/gcb.12417, 2014.

Schuur, E. A., McGuire, A. D., Schädel, C., Grosse, G., Harden, J. W., Hayes, D. J., Hugelius, G., Koven, C. D., Kuhry, P., Lawrence, D. M.: Climate change and the permafrost carbon feedback. Nature., 520, 171-179, https://doi.org/10.1038/nature14338, 2015.

Schuur, E. A., Vogel, J. G., Crummer, K. G., Lee, H., Sickman, J. O., Osterkamp, T.: The effect of permafrost thaw on old carbon release and net carbon exchange from tundra. Nature., 459, 556-559, https://doi.org/10.1038/nature08031, 2009.

Sinsabaugh, R. L., Lauber, C. L., Weintraub, M. N., Ahmed, B., Allison, S. D., Crenshaw, C., Contosta, A. R., Cusack, D., Frey, S., Gallo, M. E.: Stoichiometry of soil enzyme activity at global scale. Ecology letters., 11, 1252-1264, https://doi.org/10.1111/j.1461-0248.2008.01245.x, 2008.

Sinsabaugh, R. L., Manzoni, S., Moorhead, D. L., Richter, A.: Carbon use efficiency of microbial communities: stoichiometry, methodology and modelling. Ecology letters., 16, 930-939, https://doi.org/10.1111/ele.12113, 2013.

Sokol, N. W., Sanderman, J., Bradford, M. A.: Pathways of mineral-associated soil organic matter formation: Integrating the role of plant carbon source, chemistry, and point of entry. Global Change Biology., 25, 12-24, https://doi.org/10.1111/gcb.14482, 2019.

Stanford, G., Smith, S.: Nitrogen mineralization potentials of soils. Soil Science Society of America Journal., 36, 465-472, https://doi.org/10.2136/sssaj1972.03615995003600030029x, 1972.

Štursová, M., Žifčáková, L., Leigh, M. B., Burgess, R., Baldrian, P.: Cellulose utilization in forest litter and soil: identification of bacterial and fungal decomposers. FEMS microbiology ecology., 80, 735-746, https://doi.org/10.1111/j.1574-6941.2012.01343.x, 2012.

Symonds, M. R., Moussalli, A.: A brief guide to model selection, multimodel inference and model averaging in behavioural ecology using Akaike's information criterion. Behavioral ecology and

https://doi.org/10.5194/egusphere-2026-3656
Preprint. Discussion started: 9 July 2026

711 sociobiology., 65, 13-21, https://doi.org/10.1007/s00265-010-1037-6, 2011.
712 Tukey, J. W.: Comparing individual means in the analysis of variance. Biometrics., 99-114,
713 https://doi.org/10.2307/3001913, 1949.
714 Turetsky, M. R., Abbott, B. W., Jones, M. C., Anthony, K. W., Olefeldt, D., Schuur, E. A., Grosse, G.,
715 Kuhry, P., Hugelius, G., Koven, C.: Carbon release through abrupt permafrost thaw. Nature
716 Geoscience., 13, 138-143, https://doi.org/10.1038/s41561-019-0526-0, 2020.
717 Walker, L. R., Wardle, D. A., Bardgett, R. D., Clarkson, B. D.: The use of chronosequences in studies of
718 ecological succession and soil development. Journal of ecology., 98, 725-736,
719 https://doi.org/10.1111/j.1365-2745.2010.01664.x, 2010.
720 Wang, W., Dalal, R., Moody, P., Smith, C.: Relationships of soil respiration to microbial biomass,
721 substrate availability and clay content. Soil biology and biochemistry., 35, 273-284,
722 https://doi.org/10.1016/s0038-0717(02)00274-2, 2003.
723 Werth, M., Kuzyakov, Y.: 13C fractionation at the root–microorganisms–soil interface: a review and
724 outlook for partitioning studies. Soil Biology and Biochemistry., 42, 1372-1384,
725 https://doi.org/10.1016/j.soilbio.2010.04.009, 2010.
726 Wieder, W. R., Bonan, G. B., Allison, S. D.: Global soil carbon projections are improved by modelling
727 microbial processes. Nature climate change., 3, 909-912, https://doi.org/10.1038/nclimate1951,
728 2013.
729 Wold, H.: Soft modeling: the basic design and some extensions. Systems under indirect observation, Part
730 II 2: 36-37, 1982.
731 Zak, D. R., Pregitzer, K. S., Burton, A. J., Edwards, I. P., Kellner, H.: Microbial responses to a changing
732 environment: implications for the future functioning of terrestrial ecosystems. Fungal Ecology., 4,
733 386-395, https://doi.org/10.1016/j.funeco.2011.04.001, 2011.
734